Structures and Magnetic Properties of Iron(III) Dinuclear Complexes with Alkoxo and Carboxylato Bridges

Masako Kato,*[1a] Yasuko Yamada,[1a] Tomoko Inagaki,[1a] Wasuke Mori,[1b] Ken Sakai,[1c] Taro Tsubomura,[1c] Mitsunobu Sato,[1d] and Shigenobu Yano*[1a]

Department of Chemistry, Faculty of Science, Nara Women's University, Nara 630, Japan, Department of Chemistry, Faculty of Science, Osaka University, Toyonaka, Osaka 560, Japan, Department of Chemistry, Faculty of Engineering, Seikei University, Musashino, Tokyo 180, Japan, and Department of General Chemistry, Faculty of Engineering, Kogakuin University, Hachioji, Tokyo 192, Japan

Received February 9, 1994[⊗]

A series of diiron(III) complexes containing alkoxo and carboxylato bridges, $[Fe_2(dhpta)(OOCR)(H_2O)_2]$ (H_5-dhpta = 1,3-diamino-2-hydroxypropane-*N,N,N′,N′*-tetraacetic acid; R = C_6H_4OH (**1**), $CH_2CH{=}CH_2$ (**2**), C_6H_4-NH_2 (**3**), CH_2CH_2Br (**4**); $CH{=}CHCH_3$ (**5**)) have been synthesized. Their molecular structures and magnetic properties were investigated. For **1** and **2**, the crystal structures have been determined by X-ray analysis. Crystal data: for **1**, dihydrate, triclinic, $P\bar{1}$, a = 9.929(3) Å, b = 18.955(6) Å, c = 7.862(2) Å, α = 113.60(2)°, β = 107.57(2)°, γ = 61.79(3)°, V = 1182.2(7) Å^3, Z = 2, R = 0.050; for **2**, triclinic, $P\bar{1}$, a = 10.020(1) Å, b = 15.952(1) Å, c = 6.7523(7) Å, α = 95.536(7)°, β = 97.968(8)°, γ = 86.612(7)°, V = 1062.7(2) Å^3, Z = 2, R = 0.050. For both complexes, two Fe(III) ions take rather distorted octahedral structure and are bridged by the alkoxyl group of dhpta and the carboxylate ion. Fe−O(R) distances are 2.006(2) and 1.985(2) Å for **1** and 1.971(4) and 1.998(3) Å for **2**, and the Fe−O(R)−Fe angle is 130.0(1)° for **1** and 130.2(2)° for **2**. EXAFS, XANES, and IR data support that all the complexes have similar (μ-alkoxo)(μ-carboxylato)diiron dimer structures. Independent of the bridging carboxylate ligand, all these complexes exhibit similar weak antiferromagnetic exchange interactions between the spins of the ferric ions through the O(−R) bridge ($-J$ = 14−16 cm^{-1}). Among these complexes, a small but significant increase in the $-J$ value with shorter Fe−(μ-O) distance is noted. This indicates that the spin exchange interaction is very sensitive to the bond length between Fe and bridging oxygen atoms also for the (μ-alkoxo)diiron(III) complexes. Both **1** and **2** have the crystal structures with a separate arrangement of hydrophilic and hydrophobic parts and stacking of the π system.

Introduction

Many dinuclear Fe(III) complexes bridged by oxygen atoms have been extensively synthesized and investigated from the viewpoint of biological model complexes and/or their interesting physical properties.[2,3] They exhibit characteristic antiferromagnetic exchange interactions between the spins on two ferric ions through the O-bridge. It is a general feature that the exchange interactions are much stronger for μ-oxo complexes ($-J$ = 80−120 cm^{-1}) than for μ-hydroxo complexes ($-J$ = 7−17 cm^{-1}) and alkoxo-bridged diiron complexes exhibit comparable J values to μ-hydroxo dimers.[4−6a] No clear explanation of these trends has been given yet. As a weak coupling model, it is necessary to investigate more examples of the (μ-alkoxo)diiron complexes systematically. Much effort has been made to synthesize new types of (μ-alkoxo)diiron complexes as well as μ-phenoxo complexes using several multidentate bridging ligands.[6] 1,3-Diamino-2-hydroxypropane-*N,N,N′,N′*-tetraacetic acid, H_5dhpta, is one of the good bridging ligands, and a tetranuclear complex with oxo and carbonato bridges besides the alkoxo bridge[7] and a dimer complex containing a benzoato bridge were reported.[8]

In this paper, we have newly synthesized a series of (dhpta)iron(III) dimers with a bridging carboxylate ion, $[Fe_2(dhpta)(OOCR)(H_2O)_2]$ (R = C_6H_4OH, **1**; R = CH_2-$CH{=}CH_2$, **2**; R = $C_6H_4NH_2$, **3**; R = CH_2CH_2Br, **4**; R = $CH{=}CHCH_3$, **5**) and investigated their molecular structures and magnetic properties. Weak antiferomagnetic interactions were found independent of the bridging carboxylate ions. For the complexes, **1** and **2**, the crystal structures were determined by X-ray crystallography, and for all other complexes, the molecular structures were deduced by extended X-ray absorption fine structure (EXAFS) and X-ray absorption near-edge structure (XANES). We also report on the interesting crystal structures of **1** and **2** with separate arrangement of hydrophobic and hydrophilic parts and stacking of the π-system.

⊗ Abstract published in *Advance ACS Abstracts,* April 15, 1995.

(1) (a) Nara Women's University. (b) Osaka University. (c) Seikei University. (d) Kogakuin University.
(2) Kurtz, D. M. J. *Chem. Rev.* **1990**, *90*, 585.
(3) Vincent, J. B.; Olivier-Lilley, G. L.; Averill, B. A. *Chem. Rev.* **1990**, *90*, 1447.
(4) Walker, J. D.; Poli, R. *Inorg. Chem.* **1990**, *29*, 756.
(5) Chiari, B.; Piovesana, O.; Tarantelli, T.; Zanazzi, P. F. *Inorg. Chem.* **1984**, *23*, 3398; **1982**, *21*, 1396.
(6) (a) Ménage, S.; Que, L., Jr. *Inorg. Chem.* **1990**, *29*, 4293. (b) Menage, S.; Brennan, B. A.; Juarez-Garcia, C.; Münck, E.; Que, L., Jr. *J. Am. Chem. Soc.* **1990**, *112*, 6423. (c) Chen, Q.; Lynch, J. B.; Gomez-Romero, P.; Ben-Hussein, A.; Jameson, G. B.; O'Connor, C. J.; Que, L., Jr. *Inorg. Chem.* **1988**, *27*, 2673. (d) Bertrand, J. A.; Eller, P. G. *Inorg. Chem.* **1974**, *13*, 929. (e) Krebs, B.; Schepers, K.; Bremer, B.; Henkel, G.; Althaus, E.; Müller-Warmuth, W.; Griesar, K.; Haase, W. *Inorg. Chem.* **1994**, *33*, 1907. (f) Ming, L.-J.; Jang, H. G.; Que, L., Jr. *Inorg. Chem.* **1992**, *31*, 359. (g) Murch, B. P.; Bradley, F. C.; Que, L., Jr. *J. Am. Chem. Soc.* **1986**, *108*, 5027. (h) Suzuki, M.; Oshio, H.; Uehara, A.; Endo, K.; Yanaga, M.; Kida, S.; Saito, K. *Bull. Chem. Soc. Jpn.* **1988**, *61*, 3907.
(7) Jameson, D. L.; Xie, C.-L.; Hendrickson, D. N.; Potenza, J. A.; Schugar, H. J. *J. Am. Chem. Soc.* **1987**, *109*, 740.
(8) Kawata, S.; Nakamura, M.; Yamashita, Y.; Asai, K.; Kikuchi, K.; Ikemoto, I.; Katada, M.; Sano, H. *Chem. Lett* . **1992**, 135.

0020-1669/95/1334-2645$09.00/0

Experimental Section

Materials. $Fe(NO_3)_3 \cdot 9H_2O$ and a variety of carboxylic acids, RCOOH (R = C_6H_5, C_6H_4OH, $CH_2CH{=}CH_2$, $C_6H_4NH_2$, CH_2CH_2Br, $CH{=}CHCH_3$) were purchased from Wako Pure Chemical Industries, Ltd. 1,3-diamino-2-hydroxypropane-*N,N,N',N'*-tetraacetic acid (H_5-dhpta) was purchased from Tokyo Kasei Kogyo, Ltd.

Preparations of $[Fe_2(dhpta)(OOCR)(H_2O)_2]$ (R = C_6H_4OH, 1; R = $CH_2CH{=}CH_2$, 2; R = $C_6H_4NH_2$, 3; R = CH_2CH_2Br, 4; R = $CH{=}CHCH_3$, 5). The dinuclear Fe(III) complexes were prepared by a method similar to that of Kawata et al.[8] by using the corresponding carboxylic acids. Ferrous nitrate, $Fe(NO_3)_3 \cdot 9H_2O$ (5 mmol), and H_5-dhpta (2.5 mmol) were dissolved in 50 mL of water at about 70 °C, and then RCOOH (5 mmol) was added. After the solution was left to stand at room temperature for a few days, the deposited crystalline product was collected and washed with small amounts of water, acetone, and ether. **1**: 0.5 hydrate, orange-red crystal, yield 50.2%. Anal. Calcd for $Fe_2O_{14.5}N_2C_{18}H_{23}$: C, 35.38; H, 3.79; N, 4.58. Found: C, 35.28; H, 3.82; N, 4.58. IR (KBr, cm^{-1}): 1641, 1341 (bridging COO), 1505, 1360 (unidentate COO). **2**: yellow crystal, yield 50.2%. Anal. Calcd for $Fe_2O_{13}N_2C_{15}H_{22}$: C, 32.75; H, 4.03; N, 5.09. Found: C, 32.65; H, 3.83; N, 5.17. IR (KBr, cm^{-1}): 1631, 1323 (bridging COO), 1440, 1366 (unidentate COO). **3**: black crystal, yield 84.1%. Anal. Calcd for $Fe_2O_{15}N_3C_{18}H_{28}$: C, 33.93; H, 4.27; N, 6.60. Found: C, 33.89; H, 4.23; N, 6.53. IR(KBr, cm^{-1}): 1642,1336 (bridging COO), 1483, 1373 (unidentate COO). **4**: yellow crystal, yield 35.0%. Anal. Calcd for $Fe_2BrO_{13}N_2C_{14}H_{21}$: C, 27.26; H, 3.43 N, 4.54. Found: C, 27.19; H, 3.54; N, 4.53. IR (KBr, cm^{-1}): 1631, 1324 (bridging COO), 1449, 1367 (unidentate COO). **5**: yellow crystal, yield 48.8%. Anal. Calcd for $Fe_2O_{14.5}N_2C_{15}H_{25}$: C, 31.22; H, 4.28; N, 4.85. Found: C, 31.14; H, 4.20; N, 4.93. IR (KBr, cm^{-1}): 1641, 1339 (bridging COO), 1510, 1371 (unidentate COO).

Physical Measurements. Infrared spectra were recorded as KBr pellets on a Perkin-Elmer 1740 spectrometer.

Magnetic susceptibility data were measured by the Faraday method over a temperature range 4−300 K with a Cahn RH electrobalance. Magnetic susceptibilities at room temperature were also obtained by the Gouy method. The diamagnetism of the complexes was corrected from Pascal's constants.[9] The temperature dependence of the molar susceptibility was analyzed by using the van Vleck equation with the eigenvalues of the spin coupling Hamiltonian ($H = -2JS_1 \cdot S_2$, $S_1 = S_2 = {}^5/_2$). All the data were fit to the modified van Vleck equation by adding a temperature-independent paramagnetism (TIP) term as shown in eq 1,[10] where $x = -J/kT$, N = Avogadro's number, β = Bohr magneton, and k = Boltzman's constant.

$$\chi_m(\text{per ion}) = \frac{Ng^2\beta^2}{kT}\frac{55 + 30e^{10x} + 14e^{18x} + 5e^{24x} + e^{28x}}{11 + 9e^{10x} + 7e^{18x} + 5e^{24x} + 3e^{28x} + e^{30x}} + \text{TIP} \quad (1)$$

EXAFS and XANES spectra were collected at Beam Line 6B with a Si(111) monochromator and Beam Line 10B with a Si(311) channel-cut monochromator at the Photon Factory of the National Laboratory for High Energy Physics (2.5 GeV, 290 mA). The data were obtained on polyethylene diluted pellets (ϕ 13 mm) at ambient temperature by the method described previously.[11] The absorption spectra were recorded as a function of the X-ray photon energy with an integration time of 2 s/point at BL-6B and 1 s/point at BL-10B, with 780 steps covering the Fe K-edge (6561−8111 eV).

These data were analyzed by using the program EXAFS1 by Kosugi et al.[12] on a HITAC M-680H at the Computer Center of the University of Tokyo. After background subtraction by fitting a forth-order polynomial and subtracting it from the data, the modulation χ of the X-ray absorption coefficient was extracted with a three region cubic-spline function. The X-ray photon energy E was converted into the photoelectron wave vector k defined by $[(2m/\hbar^2)(E - E_0)]^{1/2}$, where m is the electron mass, $\hbar$ is Plank's constant divided by 2π, and E_0 is the threshold energy (7123 eV), and then the data were normalized. Nonlinear least-squares curve-fitting to the k^3-weighted $\chi(k)$ data was performed with empirical back-scattering amplitude and phase shift parameters.[13] The complex **1** was used as a model to determine these parameters for Fe−(O/N), Fe−C, and Fe−Fe. Averaged values of the interatomic distances found in the crystal structure were used as the input data for each shell (see Table 5). Fourier transforms and curve-fitting to the $k^3\chi(k)$ data for all the complexes were performed over the range of 4−14 $Å^{-1}$. The R range in the back-transforms from R to k space was 0.97−3.67 Å. Nine parameters, N_i, r_i, and the Debye−Waller factor, σ_i, (i = 1−3), were varied while E_0 was fixed in the curve-fitting.

Table 1. Crystallographic Parameters for $[Fe_2(dhpta)(OOCC_6H_4OH)(H_2O)_2] \cdot 2H_2O$ (**1**) and $[Fe_2(dhpta)(OOCCH_2CH{=}CH_2)(H_2O)_2]$ (**2**)

	1	**2**
formula	$Fe_2O_{14}N_2C_{18}H_{22} \cdot 2H_2O$	$Fe_2O_{13}N_2C_{15}H_{22}$
fw	638.11	550.04
cryst system	triclinic	triclinic
α/deg	113.60(2)	95.536(7)
β/deg	107.57(2)	97.968(8)
γ/deg	61.79(3)	86.612(7)
V/Å^3	1182.2(7)	1062.7(2)
Z	2	2
ϱ_{calcd}/g cm^{-3}	1.79	1.72
cryst size/mm	0.26 × 0.23 × 0.12	0.20 × 0.30 × 0.03
scan range	1.2 + 0.5 tan θ	1.21 + 0.3 tan θ
μ(Mo Kα)/mm^{-1}	1.24	1.43
2θ range/deg	2−60	3−55
no. of data ($I > 3\sigma(I)$)	5353	3036
no. of variables	448	289
R^a	0.050	0.050
$R_w{}^b$	0.059	0.042

$^a R = \sum||F_o| - |F_c||/\sum|F_o|$. $^b R_w = [\sum w(|F_o| - |F_c|)^2/\sum w|F_o|^2)]^{1/2}$.

The X-ray diffraction data of the complexes **1** and **2** were obtained at room temperature on a Rigaku AFC-6B and AFC-5S four-circle diffractometers, respectively, with use of graphite-monochromated Mo Kα radiation. An orange-red plate crystal of **1** (0.26 × 0.23 × 0.06 mm) and a yellow prismatic crystal of **2** (0.20 × 0.10 × 0.10 mm) were mounted on glass fibers. The $\theta-2\theta$ scan mode was used at a scan rate of 4° min^{-1} for **1** and 8° min^{-1} for **2** to record the intensities. The intensities of three standard reflections were monitored at 100-reflection intervals. Fluctuations for the F_o values were less than 2% during the data collection. Index ranges are as follows: $-13 \le h \le 13$, $-26 \le k \le 26$, $0 \le l \le 11$ for **1**; $0 \le h \le 13$, $-21 \le k \le 21$, $-9 \le l \le 9$ for **2**. The intensity data were corrected for Lorenz−polarization effects. Absorption corrections were applied with a numerical integration procedure with a Gaussian grid (6 × 6 × 6) for **1** and with an empirical method based on azimuthal scans of several reflections for **2**. Pertinent crystallographic parameters are summarized in Table 1.

For **1**, the structure was solved and refined by the standard Patterson, Fourier, and block-diagonal least-squares techniques. The atomic scattering factors for non-hydrogen and hydrogen atoms were taken from the literature.[14,15] Non-hydrogen atoms were refined anisotropically. Further difference syntheses permitted location of the hydrogen atoms, and they were included in the final refinement with isotropic temperature factors. The final R indices are listed in Table 1. The weighting scheme employed was $w = [\sigma^2(|F_o|) + (0.015|F_o|^2]^{-1}$. A final difference-Fourier synthesis showed no unusual features with $\Delta\varrho_{max} = 1.03$ e/Å^3. The calculations were carried out on the Fujitsu M77016 computer at the Information Processing Center of the Nara

(9) Foex, G. *Constants Sélectionées, Diamagnétisme et Paramagnétisme*; Masson: Paris, 1957.
(10) Wojciechowski, W. *Inorg. Chim. Acta* **1967**, *1*, 319.
(11) Tanase, T.; Nouchi, R.; Oka, Y.; Kato, M.; Nakamura, N.; Yamamura, T.; Yamamoto, Y.; Yano, S. *J. Chem. Soc., Dalton Trans.* **1993**, 2645.
(12) Kosugi, N.; Kuroda, H. *Program EXAFS 1*; Research Center for Spectrochemistry, The University of Tokyo: Tokyo, Japan, 1985.
(13) Cramer, S. P.; Eccles, T. K.; Kutzler, F.; Hodgson, K. O.; Doniach, S. *J. Am. Chem. Soc.* **1976**, *98*, 8059.
(14) *International Tables for X-ray Crystallography*; Kynoch Press: Birmingham, England, 1974; Vol. IV.
(15) Stewart, R. F.; Davidson, E. R.; Simpson, W. T. *J. Chem. Phys.* **1965**, *42*, 3175.

Table 2. Atomic Coordinates ($\times 10^4$) and Thermal Parameters (Å^2) for the Non-Hydrogen Atoms of $[Fe_2(dhpta)(OOCC_6H_4OH)(H_2O)_2]\cdot 2H_2O$ (**1**)

atom	x	y	z	B_{eq}[a]
Fe(1)	−1504(1)	3170(0)	259(1)	1.4(1)
Fe(2)	2640(1)	2013(0)	838(1)	1.3(1)
O(1)	−1084(3)	4194(2)	1392(3)	1.9(1)
O(2)	−1620(4)	5438(2)	1180(5)	4.2(1)
O(3)	−2618(3)	2481(2)	−1568(4)	2.4(1)
O(4)	−4214(4)	2278(2)	−4180(4)	4.2(1)
O(5)	598(3)	2554(1)	−546(3)	1.5(1)
O(6)	2923(3)	3084(1)	2079(3)	1.8(1)
O(7)	4421(3)	3708(2)	2361(4)	2.5(1)
O(8)	3194(3)	839(2)	−914(4)	2.0(1)
O(9)	4704(3)	−178(2)	−3050(4)	2.6(1)
O(10)	−3540(3)	3980(2)	1378(4)	2.3(1)
O(11)	4765(3)	1540(2)	2330(4)	2.1(1)
O(12)	−867(3)	2521(2)	1976(4)	2.1(1)
O(13)	1688(3)	1859(2)	2410(4)	2.0(1)
O(14)	−156(4)	−852(2)	2590(5)	3.6(2)
O(15)	−3011(4)	5076(3)	4490(5)	5.2(2)
O(16)	170(5)	4133(3)	−4769(5)	5.3(1)
N(1)	−2120(3)	3588(2)	−2187(4)	1.9(1)
N(2)	3506(3)	2050(2)	−1370(4)	1.5(1)
C(1)	−1638(4)	4737(2)	497(5)	2.3(1)
C(2)	−2366(5)	4481(2)	−1505(6)	2.8(1)
C(3)	−3475(4)	3421(3)	−3317(5)	2.7(1)
C(4)	−3440(4)	2660(3)	−3061(5)	2.6(1)
C(5)	−749(4)	3035(2)	−3191(5)	2.0(1)
C(6)	718(4)	2895(2)	−1812(4)	1.6(1)
C(7)	2122(4)	2266(2)	−2790(5)	1.9(1)
C(8)	3824(4)	3200(2)	1455(5)	1.8(1)
C(9)	4164(4)	2688(2)	−535(5)	2.0(1)
C(10)	4639(4)	1191(2)	−2155(5)	2.0(1)
C(11)	4150(4)	557(2)	−2069(5)	1.9(1)
C(12)	352(4)	1901(2)	2275(4)	1.6(1)
C(13)	199(4)	1211(2)	2505(4)	1.6(1)
C(14)	1512(4)	540(2)	2961(5)	2.0(1)
C(15)	1373(4)	−133(2)	3038(6)	2.5(1)
C(16)	−64(5)	−163(2)	2594(5)	2.4(1)
C(17)	−1370(4)	507(3)	2180(7)	2.9(1)
C(18)	−1233(4)	1187(2)	2143(6)	2.5(1)

[a] $B_{eq} = {}^8/_3\ \pi^2(U_{11}(aa^*)^2 + U_{22}(bb^*)^2 + U_{33}(cc^*)^2 + 2U_{12}aa^*bb^* \cos\gamma + 2U_{13}aa^*cc^* \cos\beta + 2U_{23}bb^*cc^* \cos\alpha)$.

women's University with the universal crystallographic computation program system UNICS III.[16]

The structure of **2** was solved by direct methods and expanded using Fourier and full-matrix least squares techniques. The non-hydrogen atoms were refined anisotropically, and the hydrogen atoms were included but not refined. Neutral atom scattering factors were taken from the literature.[14] Anomalous dispersion effects were included in F_c;[17] the values for $\Delta f'$ and $\Delta f''$ were those of Creagh and McAuley.[18] The calculations were performed using the TEXAN crystallographic software package.[19] The weight was taken as $w = [\sigma^2(|F_o|)]^{-1}$. A final difference-Fourier synthesis showed no unusual features with $\Delta\varrho_{max} = 0.57$ e/Å^3. Positional and thermal parameters for the non-hydrogen atoms of **1** and **2** are given Tables 2 and 3, respectively.

Results and Discussion

A series of (μ-alkoxo)(μ-carboxylato)diiron(III) complexes have been synthesized easily by the reaction of ferric ion with H_5dhpta and a variety of carboxylic acids. All the newly synthesized Fe(III) complexes were proven to have the com-

Table 3. Atomic Coordinates ($\times 10^4$) and Thermal Parameters (Å^2) for the Non-Hydrogen Atoms of $[Fe_2(dhpta)(OOCCH_2CH{=}CH_2)(H_2O)_2]$ (**2**)

atom	x	y	z	B_{eq}[a]
Fe(1)	5394.5(8)	1735.8(5)	3050(1)	1.90(3)
Fe(2)	8177.4(8)	3110.6(5)	4106(1)	2.16(3)
O(1)	4392(4)	2394(2)	5048(5)	2.2(1)
O(2)	2434(4)	3007(3)	5666(6)	3.5(2)
O(3)	5579(4)	1086(2)	421(5)	2.6(1)
O(4)	4508(4)	643(2)	−2575(6)	3.4(2)
O(5)	6428(3)	2706(2)	2650(5)	2.0(1)
O(6)	7282(4)	3822(3)	6124(5)	2.8(2)
O(7)	6545(6)	5111(3)	7157(7)	5.6(2)
O(8)	9236(4)	2910(3)	1827(6)	3.5(2)
O(9)	10178(5)	3487(4)	−474(7)	6.4(2)
O(10)	4132(4)	772(2)	3430(5)	2.4(2)
O(11)	9939(3)	3599(2)	5689(5)	2.4(1)
O(12)	6840(4)	1230(3)	4867(6)	3.3(2)
O(13)	8567(4)	2072(3)	5449(7)	4.1(2)
N(1)	3808(4)	2345(3)	1068(6)	1.8(2)
N(2)	7593(5)	4221(3)	2474(7)	2.5(2)
C(1)	3199(6)	2701(3)	4503(8)	2.2(2)
C(2)	2723(5)	2681(4)	2268(8)	2.4(2)
C(3)	3382(6)	1691(4)	−571(8)	2.5(2)
C(4)	4571(6)	1101(4)	−972(8)	2.5(3)
C(5)	4492(6)	3026(3)	275(8)	2.3(2)
C(6)	5563(6)	3386(4)	1868(8)	2.4(2)
C(7)	6414(6)	3967(4)	1010(8)	2.5(2)
C(8)	6984(6)	4614(4)	5920(10)	3.1(3)
C(9)	7233(7)	4917(4)	3950(9)	3.7(3)
C(10)	8748(6)	4366(4)	1428(9)	3.7(3)
C(11)	9433(6)	3536(5)	831(9)	4.1(2)
C(12)	7961(7)	1445(4)	5811(10)	3.3(3)
C(13)	8582(7)	917(5)	7450(10)	5.6(4)
C(14)	10061(9)	850(6)	7650(10)	7.9(3)
C(15)	10803(10)	120(6)	7700(20)	8.7(3)

[a] $B_{eq} = {}^8/_3\ \pi^2(U_{11}(aa^*)^2 + U_{22}(bb^*)^2 + U_{33}(cc^*)^2 + 2U_{12}aa^*bb^* \cos\gamma + 2U_{13}aa^*cc^* \cos\beta + 2U_{23}bb^*cc^* \cos\alpha)$.

position of Fe:dhpta:carboxylate:H_2O = 2:1:1:2 from the analytical data. IR data of all the complexes indicate the existence of a bridging carboxyl group besides those for unidentate acetate groups in dhpta^{5-} (see Experimental Section).

Molecular Structures of 1 and 2. Figures 1 and 2 show the ORTEP drawings of **1** and **2**, respectively. In both complexes, the dhpta^{5-} ligand binds to two Fe(III) ions bridging with the alkoxy oxygen and the bridging carboxylate ion and two waters occupy the *trans* positions of the alkoxo bridge and N atoms, respectively. They are the same dimeric structures as that of $[Fe_2(dhpta)(OOCC_6H_5)(H_2O)_2]\cdot 2H_2O$ reported recently.[8] Table 4 lists relevant interatomic distances and angles for **1** and **2** with those data for $[Fe_2(dhpta)(OOCC_6H_5)(H_2O)_2]\cdot 2H_2O$. Each Fe(III) ion takes a distorted octahedral structure. Especially, it is noticeable that the Fe−N bonds are fairly long (2.17−2.19 Å) and the angles of O(1)−Fe(1)−O(3) and O(6)−Fe(2)−O(8) are much smaller than 180° (Table 4). Those are due to the *trans* configuration of the acetate oxygens indicating steric constraint. Similar features can be seen in the coordination structure of the tetranuclear complex with dhpta^{5-}.[7] We have found the facial coordination of the acetate arms of dhpta (*i.e. cis* configuration) in a (μ-alkoxo)bis(μ-carboxylato)-diruthenium complex, $[Ru_2(dhpta)(OOCCH_3)_2]^-$, which is the first example of a structurally characterized ruthenium analogue of hemerythrin models with a μ-alkoxo bridge.[20] In the ruthenium dimer, the structural distortion around the ruthenium ions is much less than that found in these iron dimers. The

(16) Sakurai, T.; Kobayashi, K. *Rikagaku Kenkyusho Hokoku* **1979**, *55*, 69.
(17) Ibers, J. A.; Hamilton, W. C. *Acta Crystallogr.* **1964**, *17*, 781.
(18) *International Tables for Crystallography*; Kluwer Academic Publishers: Boston, MA, 1992; Vol. C.
(19) *TEXRAY Structural Analysis Package*; Molecular Structure Corp.: The Woodlands, TX, 1985.
(20) Tanase, T.; Kato, M.; Yamada, Y.; Tanaka, K.; Lee, K.; Sugihara, Y.; Ichimura, A.; Kinoshita, I.; Haga, M.; Sasaki, Y.; Yamamoto, Y.; Nagano, T.; Yano, S. *Chem. Lett.* **1994**, 1853.

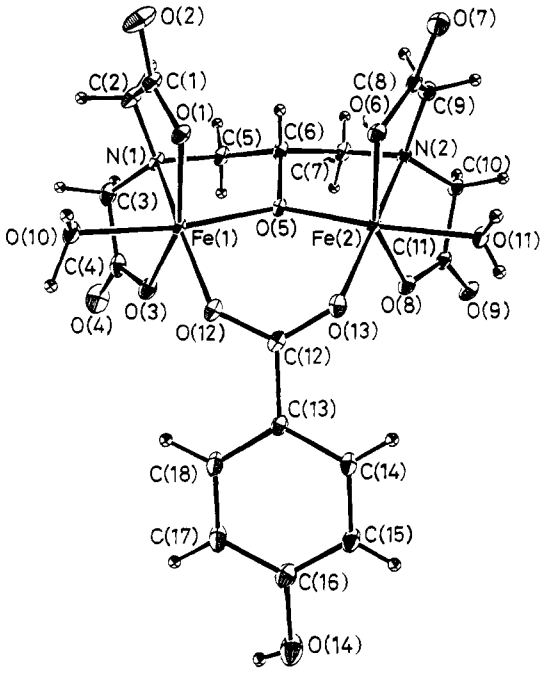

Figure 1. ORTEP drawing of $[Fe_2(dhpta)(OOCC_6H_4OH)(H_2O)_2]$ (**1**). Thermal ellipsoids are depicted at the 50% probability level.

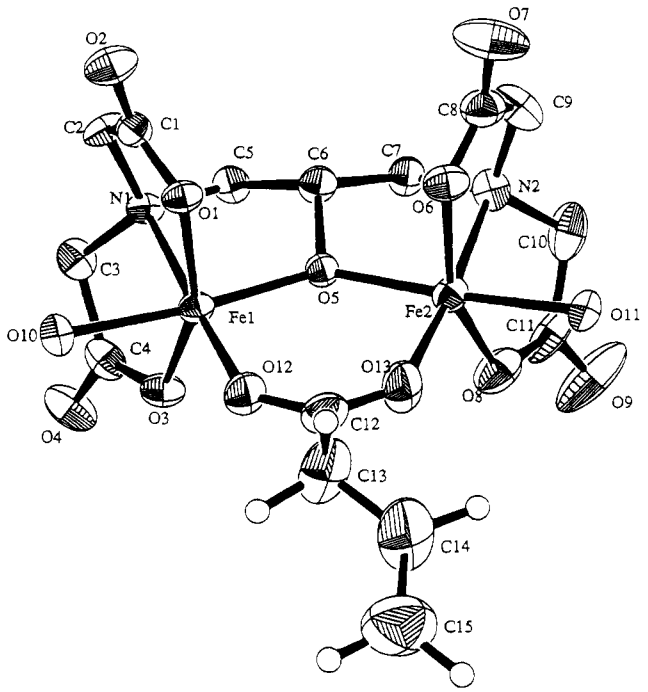

Figure 2. ORTEP drawing of $[Fe_2(dhpta)(OOCCH_2CH{=}CH_2)(H_2O)_2]$ (**2**). Thermal ellipsoids are depicted at the 50% probability level.

trans configuration of the iron dimers may depend on the synthetic conditions. It seems favorable to form a tetranuclear complex because two H_2O ligands occupy the *trans* positions to the μ-alkoxo oxygen and have a little longer Fe−O bond distances. These sites are available to the bridging sites to form a tetranuclear complex like $Na_6[Fe_4(dhpta)_2(O)_2(CO_3)_2]$.[7] In fact, we have obtained a new tetranuclear complex containing the dhpta ligand and determined the structure very recently.[21]

X-ray Absorption Spectra. In order to confirm the alkoxo-bridged diiron core on the complexes **3**−**5**, EXAFS and XANES

(21) Inagaki, T.; Yamada, Y.; Kato, M.; Tubomura, T.; Sakai, K.; Yamazaki, M.; Sato, M.; Mori, W.; Kinoshita, I.; Yano, S. Manuscript in preparation.

Table 4. Relevant Interatomic Distances (Å) and Angles (deg) for $[Fe_2(dhpta)(OOCR)(H_2O)_2]$

	R		
	C_6H_4OH (**1**)	$CH_2CH{=}CH_2$ (**2**)	C_6H_5[a]
Fe(1)−O(1)	1.973(3)	1.978(4)	1.965(5)
Fe(1)−O(3)	1.975(3)	1.993(4)	1.992(1)
Fe(1)−O(5)	2.006(2)	1.971(4)	1.986(1)
Fe(1)−O(10)	2.067(3)	2.104(4)	2.050(1)
Fe(1)−O(12)	1.952(3)	1.952(4)	1.945(2)
Fe(1)−N(1)	2.179(4)	2.177(4)	2.188(2)
Fe(2)−O(5)	1.985(2)	1.998(3)	2.006(1)
Fe(2)−O(6)	1.986(3)	1.967(4)	1.970(1)
Fe(2)−O(8)	2.000(2)	1.979(4)	1.976(1)
Fe(2)−O(11)	2.047(2)	2.085(4)	2.075(2)
Fe(2)−O(13)	1.940(4)	1.958(5)	1.969(1)
Fe(2)−N(2)	2.194(4)	2.184(5)	2.184(2)
Fe(1)···Fe(2)	3.618(2)	3.601(1)	3.608(1)
O(1)−Fe(1)−O(3)	153.6(1)	154.7(2)	
O(1)−Fe(1)−O(5)	87.8(1)	93.1(2)	
O(1)−Fe(1)−O(10)	81.9(1)	83.6(2)	
O(1)−Fe(1)−O(12)	113.5(1)	99.4(2)	
O(1)−Fe(1)−N(1)	79.5(1)	79.6(2)	77.93(6)
O(3)−Fe(1)−O(5)	102.6(1)	97.0(2)	
O(3)−Fe(1)−O(10)	87.6(1)	84.4(2)	
O(3)−Fe(1)−O(12)	90.8(1)	102.8(2)	
O(3)−Fe(1)−N(1)	77.8(1)	78.6(2)	79.12(6)
O(5)−Fe(1)−O(10)	169.6(1)	174.8(1)	
O(5)−Fe(1)−O(12)	91.0(1)	94.8(2)	91.27(5)
O(5)−Fe(1)−N(1)	83.0(1)	83.4(2)	82.52(5)
O(10)−Fe(1)−O(12)	91.2(1)	89.8(2)	90.55(5)
O(10)−Fe(1)−N(1)	97.0(1)	91.9(2)	96.34(6)
O(12)−Fe(1)−N(1)	165.6(1)	177.9(2)	
O(5)−Fe(2)−O(6)	92.7(1)	92.7(2)	
O(5)−Fe(2)−O(8)	98.2(1)	97.3(2)	
O(5)−Fe(2)−O(11)	175.6(1)	176.5(1)	
O(5)−Fe(2)−O(13)	91.4(1)	92.6(2)	91.07(6)
O(5)−Fe(2)−N(2)	83.0(1)	82.7(2)	82.86(6)
O(6)−Fe(2)−O(8)	152.8(1)	154.2(2)	
O(6)−Fe(2)−O(11)	83.0(1)	84.2(2)	
O(6)−Fe(2)−O(13)	110.0(1)	100.8(2)	
O(6)−Fe(2)−N(2)	79.4(1)	79.8(2)	78.05(5)
O(8)−Fe(2)−O(11)	85.5(1)	85.0(2)	
O(8−Fe(2)−O(13)	94.6(1)	102.4(2)	
O(8)−Fe(2)−N(2)	77.4(1)	78.0(2)	78.88(5)
O(11)−Fe(2)−O(13)	90.7(1)	89.5(2)	90.07(6)
O(11)−Fe(2)−N(2)	95.5(1)	95.2(2)	97.68(6)
O(13)−Fe(2)−N(2)	169.4(1)	175.3(2)	
Fe(1)−O(5)−Fe(2)	130.0(1)	130.2(2)	129.30(7)

[a] Reference 8.

spectra of a series of $[Fe_2(dhpta)(OOCR)(H_2O)_2]$ complexes have been measured. The Fourier transforms of the k^3-weighted EXAFS data ($k^3\chi(k)$) for the complexes **1**−**5** are shown in Figure 3 with that for $[Fe_2(dhpta)(OOCC_6H_5)(H_2O)_2]$. All the Fourier transforms are very similar and show three peaks at around 1.6, 2.5, and 3.3 Å (before phase-shift correction). These are easily assigned to the peaks due to the oxygen and/or nitrogen atoms of the first coordination sphere, the nonbonded carbon atoms in the ligand, and the neighboring Fe atom, respectively. Fourier-filtered EXAFS data in the range containing these three peaks were used in the curve-fitting with empirical back-scattering amplitude and phase shift parameters derived from the complex **1** (see Experimental Section). All the calculations converged nicely with reasonable *R*-factors, and the results of the fits to the Fourier-filtered data are shown in Figure 4. Determined parameters are summarized in Table 5. For the complexes **1**, **2**, and $[Fe_2(dhpta)(OOCC_6H_5)(H_2O)_2]$, the crystal structures of which have been determined, the interatomic distances and the coordination numbers determined by the EXAFS analyses are consistent with those from the crystal

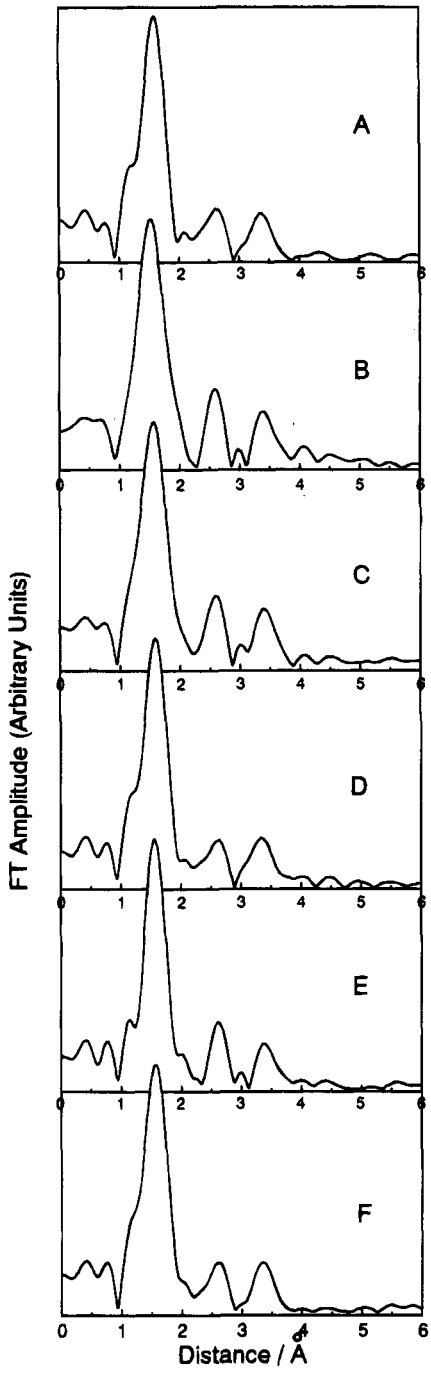

Figure 3. Fourier transforms over the range of $k = 4-14$ Å^{-1} of the k^3-weighted EXAFS data (before phase shift correction) for $[Fe_2(dhpta)(OOCR)(H_2O)_2]$ (R: (A) C_6H_5; (B) C_6H_5OH, **1**; (C) $CH_2CH{=}CH_2$, **2**; (D) $C_6H_4NH_2$, **3**; (E) CH_2CH_2Br, **4**; (F) $CH{=}CHCH_3$, **5**).

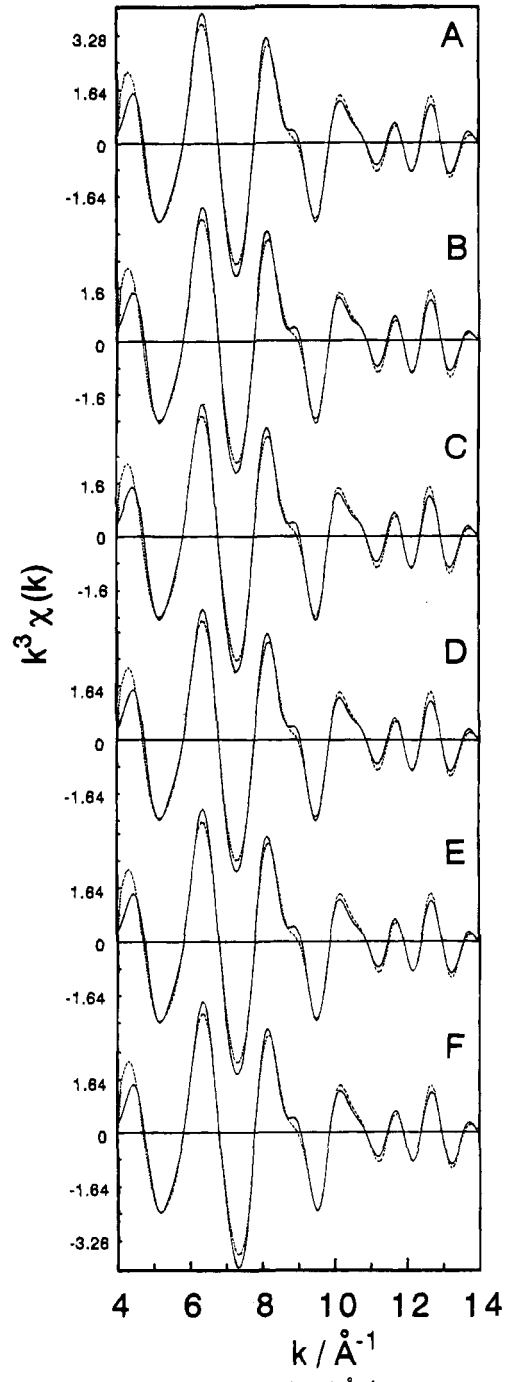

Figure 4. Fits over the range of $k = 4-14$ Å^{-1} to the Fourier filtered data for $[Fe_2(dhpta)(OOCR)(H_2O)_2]$ (R: (A) C_6H_5; (B) C_6H_5OH, **1**; (C) $CH_2CH{=}CH_2$, **2**; (D) $C_6H_4NH_2$, **3**; (E) CH_2CH_2Br, **4**; (F) $CH{=}CHCH_3$, **5**). Key: —, filtered EXAFS; - - -, least-squares fits.

structure analyses, and almost identical values were obtained for the complexes **3**–**5**. The results indicate that the structures of the complexes **3**–**5** also have the alkoxo-bridged diiron core corresponding to those of the complexes **1** and **2**, and the diiron core constructed with the dhpta ligand is proved to be rigid independent of the carboxyl bridging ligand. The coordination environments around the Fe^{3+} ion were also confirmed by XANES spectra of the complexes **1**–**5** and $[Fe_2(dhpta)(OOCC_6H_5)(H_2O)_2]$. As shown in Figure 5, all the spectra are closely similar to each other, and in every case, there is a weak peak and two strong resonances below and above the Fe K-edge ionization threshold, respectively. In the pre-edge weak peak attributable to the 1s → 3d transition[22,23] can be seen a small splitting of ca. 1.0–1.5 eV suggesting the transitions to the t_{2g} and e_g orbitals in the high-spin Fe(III) ion, respectively. The spectral profile with the weak pre-edge peak and two strong absorption bands in the post-edge region has been reported as a typical pattern for octahedral complexes such as $[Fe(CN)_6]^{4-}$ and $[Fe(CN)_6]^{3-}$.[23] Thus the XANES spectra support that all these complexes have the same coordination geometry.

Magnetic Properties. Figure 6 shows the temperature dependence of the molar susceptibility of complex **1**. This exhibits a typical behavior of antiferromagnetic interactions between Fe(III) spins with a maximum and dramatic decrease

(22) Iwai, K.; Iwai, M.; Suto, K.; Nakashima, S.; Motoyama, I.; Sano, H.; Ikemoto, I.; Kosugi, N.; Kuroda, H. *Bull. Chem. Soc. Jpn.* **1986**, *59*, 2675.
(23) Kosugi, N.; Yokoyama, T.; Kuroda, H. *Chem. Phys.* **1986**, *104*, 449.

Table 5. Atomic Parameters Determined by Curve-fitting Analysis[a] of a Series of $[Fe_2(dhpta)(OOCR)(H_2O)_2]$ Complexes

	EXAFS							X-ray cryst	
R (comp no.)	window width, Å	shell	Fe−A[b]	r, Å	N[c]	σ, Å	R[d]	r,[e] Å	N
C_6H_5	0.97−3.67	1st	Fe−O/N	2.030	6.0	0.021	0.033	2.03(8)[f]	6
		2nd	Fe−C	2.909	6.9	0.023		*f*	7
		3rd	Fe−Fe	3.619	1.0	0.049		3.608(1)	1
C_6H_4OH (**1**)	0.97−3.82	1st	Fe−O/N	2.030	6	0.020	0.034	2.03(8)	6
		2nd	Fe−C	2.909	7	0.025		2.91(6)	7
		3rd	Fe−Fe	3.621	1	0.046		3.620(2)	1
$CH_2CH{=}CH_2$ (**2**)	0.97−3.75	1st	Fe−O/N	2.030	6.0	0.021	0.034	2.03(9)	6
		2nd	Fe−C	2.909	7.0	0.024		2.92(7)	7
		3rd	Fe−Fe	3.621	1.0	0.048		3.601(1)	1
$C_6H_4NH_4$ (**3**)	0.97−3.71	1st	Fe−O/N	2.030	6.0	0.021	0.034		
		2nd	Fe−C	2.909	7.0	0.024			
		3rd	Fe−Fe	3.620	1.0	0.049			
CH_2CH_2Br (**4**)	0.97−3.71	1st	Fe−O/N	2.030	6.1	0.022	0.034		
		2nd	Fe−C	2.909	7.0	0.024			
		3rd	Fe−Fe	3.620	1.0	0.048			
$CH{=}CHCH_3$ (**5**)	0.97−3.68	1st	Fe−O/N	2.030	6.1	0.022	0.033		
		2nd	Fe−C	2.909	6.9	0.024			
		3rd	Fe−Fe	3.620	1.0	0.049			

[a] Fitting range $k = 4-14$ Å^{-1}. The number of parameters (9) is much less than the number of independent data points, $N_{idp} = 2\Delta R{\cdot}\Delta k/\pi$, where ΔR and Δk denote the window width in R-space and the fitting width in k-space, respectively. [b] Fe is the absorber and A is the back-scattering atom. [c] The coordination number referenced to that of **1**. [d] $R = [\sum(k^3\chi_o(k) - k^3\chi_c(k))^2/\sum(k^3\chi_o(k))^2]^{1/2}$, where $\chi_o(k)$ and $\chi_c(k)$ are Fourier-filtered and calculated data. [e] The values are averaged distances of crystallographic data in each shell. A number in parentheses for Fe−O/N and Fe−C is an esd for a mean value of the bond lengths and is equal to $[\sum\Delta_i^2/(n-1)]^{1/2}$, where Δ_i is the deviation of ith value in a set of n such values from the arithmetic mean of the n value. [f] Reference 8. The value of Fe−C is not available.

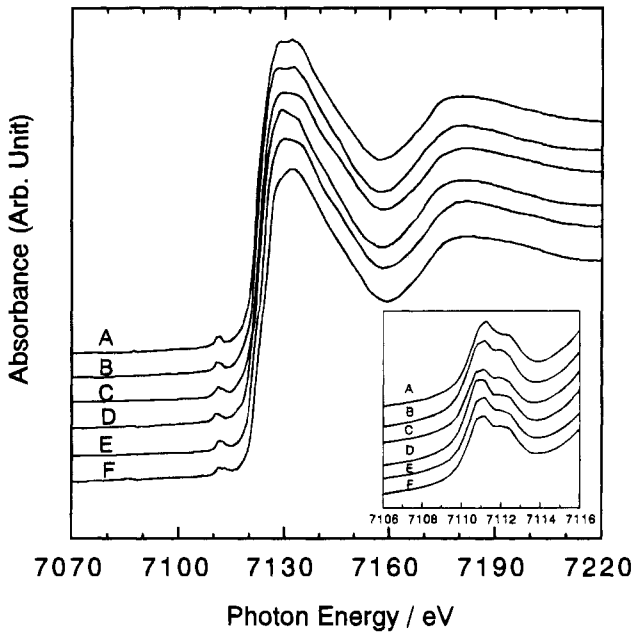

Figure 5. XANES spectra of $[Fe_2(dhpta)(OOCR)(H_2O)_2]$ (R: (A) C_6H_5; (B) C_6H_5OH, **1**; (C) $CH_2CH{=}CH_2$, **2**; (D) $C_6H_4NH_2$, **3**; (E) CH_2CH_2Br, **4**; (F) $CH{=}CHCH_3$, **5**). Inset shows the expanded spectra of the 1s → 3d region.

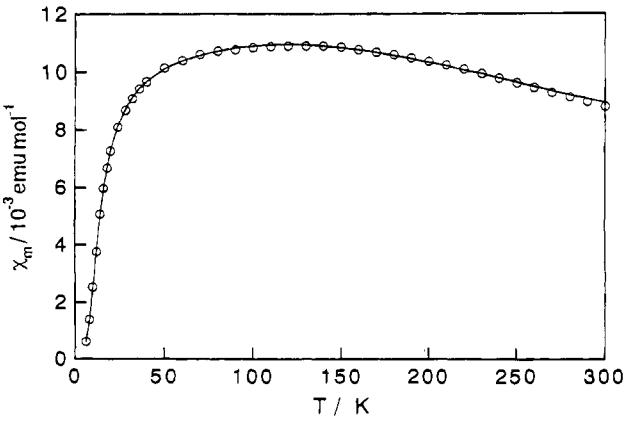

Figure 6. Temperature dependence of the magnetic susceptibility data of **1**. The solid line is calculated with use of eq 1 (see text).

of susceptibility at low temperature. These data were analyzed using an isotropic spin−spin coupling model for diiron(III) (Experimental Section). As shown in Figure 6, the calculated values (solid line) are well fitted to the observed ones. Good results were obtained also for the other complexes, and the parameters are summarized in Table 6 with the those of $[Fe_2(dhpta)(OOCC_6H_5)(H_2O)_2]$[8] and $Na_6[Fe_4(dhpta)_2(O)_2(CO_3)_2]$.[7] For all the complexes of **1**−**5**, almost the same J values (−14 to −16 cm^{-1}) were obtained, which are the normal strengths of antiferromagnetic interaction for (μ-alkoxo)diiron(III) complexes. The coupling constant J has been reported to be −11 to −26 cm^{-1} for mono- and bis(μ-alkoxo)diiron(III) complexes.[4-6] Despite the fact that the coupling must occur through the Fe−O−Fe bonds, the magnitude of J is not likely to depend on whether the complex is mono- or dibridged. Among a few mono(μ-alkoxo) complexes already reported, $[Fe_2(bhpp)(O_2P(OPh)_2)_2]BPh_4$[6e] (H$_3$bhpp = 1,3-bis[(2-hydroxybenzyl)(2-pyridylmethyl)amino]-2-propanol) has a J value of −12.5(3) cm^{-1}, whereas $[Fe_2(PTB)(O_2CPh)_2](ClO_4)_3$[6c] (HPTB = *N,N,N′,N′*-tetrakis(2-benzimidazolylmethyl)-2-hydroxy-1,3-diaminopropane) represents a larger value ($J = -26$ cm^{-1}). The X-ray structure is not yet known for the latter complex. The J values for the mono(μ-alkoxo) complexes, **1**−**5**, are in the middle positions of this range. In Table 6, the average of Fe−(μ-O) distances and Fe−O(R)−Fe angle determined by X-ray analyses are also included. A small but significant increase in the $-J$ value with shorter Fe−(μ-O) distance is noted. In contrast, there is no correlation between the $-J$ value and Fe−O−Fe angle as was pointed out for μ-oxo and μ-hydroxo complexes.[2] The result indicates that the spin exchange interaction is very sensitive to the bond length between Fe and bridging oxygen atoms also for the (μ-alkoxo)diiron(III) complexes. The antiferromagnetic coupling constant is recognized to be one of the significant parameters to deduce the core structure of the proteins containing a (μ-oxo)diiron core, such

Table 6. Comparison of Magnetic Properties of Fe(dhpta) Complexes with μ-Alkoxo Bridges

compd	(R)[a]	g	$-J$, cm^{-1}	10^6TIP, emu/mol	Fe$-(\mu$-O$)_{av}$,[b] Å	Fe$-$O$-$Fe, deg
$Na_6[Fe_4(dhpta)_2(O)_2(CO_3)_2]$[c]		2.0	11.2	800	2.05(1)	132.3(2)
	(C_6H_5)[d]	2.0	14	800	2.00(1)	129.30(7)
1	(C_6H_4OH)	1.94	14.4	380	2.00(1)	130.0(1)
2	($CH_2CH{=}CH_2$)	2.05	15.9	670	1.99(1)	130.2(2)
3	($C_6H_4NH_2$)	2.06	15.1	14		
4	(CH_2CH_2Br)	1.96	15.4	990		
5	($CH{=}CHCH_3$)	1.98	16.3	879		

[a] R denotes a substituent of $[Fe_2(dhpta)(OOCR)(H_2O)_2]$. [b] The esd in parentheses is $|q_1 - q_2|/2$, where q_1 and q_2 denote two Fe$-$O(R) distances. [c] Reference 7. [d] Reference 8.

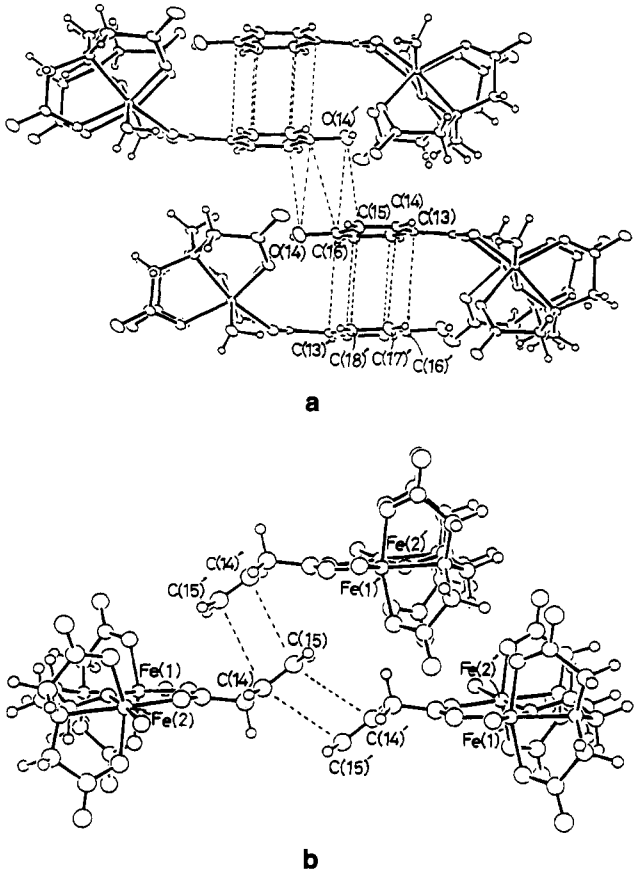

Figure 7. Molecular arrangements in the crystals: (a) $[Fe_2(dhpta)(OOCC_6H_4OH)(H_2O)_2]\cdot 2H_2O$ (**1**), C(13)$\cdots$C(16)$'$ = 3.686(5) Å, C(14)$\cdots$C(17)$'$ = 3.714(6) Å, C(15)$\cdots$C(18)$'$ = 3.743(6) Å, C(15)$\cdots$O(14)$'$ = 3.463(6) Å, C(16)$\cdots$O(14)$'$ = 3.486(5) Å, C(16)$\cdots$C(16)$'$ = 3.553(6) Å; (b) $[Fe_2(dhpta)(OOCCH_2CH{=}CH_2)(H_2O)_2]$ (**2**), C(14)$\cdots$C(15)$'$ = 3.796(8), 3.854(10) Å, C(15)$\cdots$C(15)$'$ = 3.760(5), 3.751(8) Å.

as methane monooxygenase and purple acid phosphatases. On the basis of the weak coupling constants, the existence of a μ-hydroxo or μ-alkoxo bridge instead of μ-oxo bridge is suggested for some forms of the proteins.[6a,e] Our data support the relation between the diiron core structure and J value. Menage *et al.* reported a (μ-alkoxo)diiron(II) complex, $[Fe_2(N\text{-Et-HPTB})(O_2CPh)](BF_4)_2$, with the J value of -11 cm^{-1} and the Fe$-(\mu$-O$)_{av}$ bond distance of 1.967 Å.[6b] The antiferromagnetic coupling is rather weak in spite of the short bond distances of the μ-alkoxo bridges. It is probably due to the five-coordinate structure and the divalent oxidation state of iron ions. Thus, more data from model compounds with the divalent state (Fe^{II}–Fe^{II}) and mixed-valence state (Fe^{III}–Fe^{II}) should be accumulated for further discussion of the structures of the proteins with the diiron core.

Crystal Packing of 1 and 2. It is worthwhile noticing the crystal structures of the complexes **1** and **2**. As shown in Figure 7a, the bridging hydroxy benzoates of **1** are stacked with a face-to-face configuration. The phenyl rings are precisely parallel because they are related to the inversion center and take a zigzag arrangement along the c axis keeping van der Waals contacts. The interatomic distances shown by broken thin lines in Figure 7a are 3.6–3.7 Å. Dhpta groups and coordinated water molecules form a hydrophilic network through hydrogen bonds with lattice waters (Table S1). The complex **2** also has a similar molecular arrangement in the crystal, where vinyl groups are stacked with a separation of 3.75 and 3.78 Å (Figure 7b). The dhpta ligand is likely to have a suitable size (not so bulky) so as to form such molecular arrangements with compact stacking of the π-conjugated groups in the crystal. These crystal structures suggest that the possibilities of solid phase reactions, such as photodimerization,[24] on this type of (dhpta)diiron complex.

Acknowledgment. This work was supported by a Grant-in-Aid for Scientific Research (Nos. 03555184, 05303008, 03241106, 06226102, and 06242103) from the Ministry of Education, Science, and Culture and was partially supported by a Grant-in-Aid from Iwatani Naoji Foundation's Research Grants and from Nippon Itagarasu and Mitsubishiyuka Kagaku Foundations.

Supplementary Material Available: Tables S1–S6, giving interatomic distances and angles, anisotropic thermal parameters, and hydrogen atom coordinates with isotropic thermal parameters, and Figures S1 and S2, showing packing diagrams (12 pages). Ordering information is given on any current masthead page.

IC940131Z

(24) Nakanishi, H.; Jones, N.; Thomas, J. M.; Hursthose, M. B.; Motevalli, M. *J. Phys. Chem.* **1981**, *85*, 3636.